Enhancement factor averaging and the photostability of probes in SERS vibrational pumping

P. G. Etchegoin,*[a] E. C. Le Ru,[a] R. C. Maher[b] and L. F. Cohen[b]

Received 27th April 2007, Accepted 2nd July 2007
First published as an Advance Article on the web 17th July 2007
DOI: 10.1039/b706395d

The technique of *temperature dependent vibrational pumping* in surface enhanced Raman scattering (SERS) has been recently demonstrated as a promising new tool to estimate SERS cross-sections. In this paper we expand on the previous developments and study several details around the implementation and physics of the vibrational pumping technique in SERS. Here we concentrate on two specific aspects related to: (i) the different averaging properties (over the distribution of enhancements) of the Stokes and anti-Stokes signals in the pumping regime; and (ii) the role of the finite photostability of the probes. The fact that the anti-Stokes signal is averaged differently from the Stokes counterpart leads to some unique phenomena in Raman spectroscopy that can only be observed under the conditions of vibrational pumping in SERS.

1. Preliminaries

1.1 Introduction and overview

In a recent series of papers[1–5] we have presented an in-depth discussion of vibrational pumping under surface enhanced Raman scattering (SERS)[6] conditions; including all the previous history (since its original proposal ten years ago[7]) of the search for the effect and the many problems, interpretations, and skepticism that arose along the way.[8,9] We believe the reports in ref. 1 and 2 definitely establish the technique of temperature dependent vibrational pumping (TDVP) as an additional new tool to estimate SERS cross-sections and, thereby, SERS enhancement factors.

This paper relies primarily on our previous contribution in ref. 1, where a full discussion of the many aspects of the technique has been presented. The basic idea herewith is to perfect the understanding of the method in its details, so as to achieve the best possible use of TDVP in SERS as a new tool. In addition, the purpose is to reveal basic new physics that is unique to the conditions of vibrational pumping in SERS, as we shall show later.

Along these lines, the aim here is to concentrate on two specific aspects of the vibrational pumping problem in SERS. To begin with, we show experimental evidence of the different averaging properties (over the distribution of SERS enhancements) of the Stokes and anti-Stokes signals under vibrational pumping conditions. This was predicted in ref. 1 from simple theoretical considerations, but without an experimental proof. The results in this paper justify our claim in ref. 1 that *a different averaging of the cross-section applies to the Stokes and anti-Stokes signals under SERS vibrational pumping conditions*. This also indirectly confirms the prediction that the technique yields, not the average cross-section, but a value close to (and just below) the maximum SERS cross-sections in the distribution; *i.e*. typical cross-sections seen in single molecule SERS or tip-enhanced Raman scattering (TERS).[10] In addition, the results presented in this paper will highlight the importance of the photostability of the probe in TDVP. Photobleaching of the probe can and should be avoided in TDVP, as in many other types of SERS experiments, by a careful choice of the probe, laser power, and excitation wavelength. Departing from this general principle, we choose here conditions where the limited photostability of the probe is used to evidence the different averaging conditions of the signals and the effect of the distribution of SERS enhancement factors. Photobleaching under SERS conditions is poorly understood in its details and the conditions of vibrational pumping are sufficiently specialized to open new additional questions on the nature of photobleaching. We shall only concentrate here on the *consequences* of the photostability of the probes and how they affect the estimates of cross-sections in SERS vibrational pumping, but we shall not dwell into the details of the photobleaching process itself. We, however, demonstrate explicitly an important aspect (which is often taken for granted): the photobleaching rate of a probe under SERS conditions is directly related to the SERS enhancement factor.

Being a continuation of our previous studies in ref. 1 and 2, we reduce the discussion of the pumping equations and the experimental details to a bare minimum, to avoid unnecessary repetition of information. We do highlight though the required equations needed to understand the basic phenomenology of the data presented here.

1.2 A brief reminder on SERS TDVP

The anti-Stokes/Stokes (aS/S) intensity ratio ($\rho = I_{aS}/I_S$) of a given mode in SERS vibrational pumping conditions is given by (see ref. 1 and 2):

$$\rho \equiv I_{aS}/I_S = An = A\left[\frac{\tau\sigma_S I_L}{\hbar\omega_L} + e^{-\hbar\omega_\nu/k_B T}\right], \qquad (1)$$

[a] *The MacDiarmid Institute for Advanced Materials and Nanotechnology, School of Chemical and Physical Sciences, Victoria University of Wellington, PO Box 600 Wellington, New Zealand*
[b] *The Blackett Laboratory, Imperial College London, Prince Consort Road UK SW7 2BW. E-mail: Pablo.Etchegoin@vuw.ac.nz. E-mail: Eric.LeRu@vuw.ac.nz*

where n is the average population of the vibrational mode (with frequency ω_ν), $A = \sigma_{aS}/\sigma_S$ is the *asymmetry factor* between the anti-Stokes (σ_{aS}) and Stokes (σ_S) cross-sections, τ is the vibrational lifetime of the mode, and I_L the laser power density, with photon energy $\hbar\omega_L$.

In reality, eqn (1) has to be averaged over the distribution of SERS enhancement factors leading to:

$$I_S = I_L\langle\sigma_S\rangle \tag{2}$$

$$I_{aS} = I_L\left[\langle\sigma_{aS}\sigma_S\rangle\frac{\tau I_L}{\hbar\omega_L} + \langle\sigma_{aS}\rangle e^{-\hbar\omega_\nu/k_BT}\right] \tag{3}$$

where $\langle\cdots\rangle$ denotes the average value. The anti-Stokes/Stokes ratio then follows:[1]

$$\rho = \frac{\langle\sigma_{aS}\rangle}{\langle\sigma_S\rangle}\left[\frac{\langle\sigma_{aS}\sigma_S\rangle}{\langle\sigma_{aS}\rangle}\tau\frac{I_L}{\hbar\omega_L} + e^{-\hbar\omega_\nu/k_BT}\right], \tag{4}$$

Either eqns (1) or (4) leads to two distinct regimes above or below a critical temperature, T_{cr}, given by:

$$T_{cr} \approx \frac{\hbar\omega_\nu}{k_B}\left[\ln\left(\frac{\hbar\omega_L}{\tau\sigma_S I_L}\right)\right]^{-1}, \tag{5}$$

which separates a *thermally dominated regime* (above T_{cr}) from a *pumping dominated regime* (below T_{cr}) (see Fig. 1). We show in what follows how the limited photostability of the probes can provide evidence for the picture described in eqn (4).

1.3 The SERS enhancement factor distribution and its averaging

On a separate development, we have recently provided a phenomenological description of the enhancement factor distribution in ref. 11 and 12, which in the presence of hot-spots is a *very skewed long-tail distribution*. This situation does not apply to cases where there are no hot-spots (like enhancements of flat surfaces, for example). The main point here is that a long-tail distribution has very different consequences for the

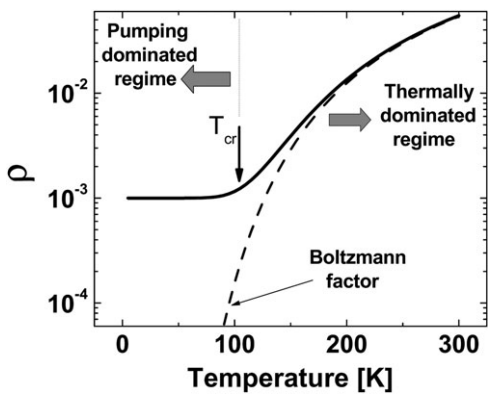

Fig. 1 If SERS vibrational pumping were not present the aS/S-ratio (ρ) would follow a normal Boltzmann factor (shown in the figure; dashed line), which decreases constantly with temperature T and accounts for the thermal population of the level. On the contrary, if pumping exists the first term in eqns (1) and (4) overtakes the second and a plateau in ρ below a critical temperature T_{cr} is observed. T_{cr} depends on laser power as shown by eqn (5) and can be shifted to higher T's if I_L is increased. This plateau plays an important role in the estimation of the cross-section *via* TDVP.[1,2]

averaging of the Stokes and anti-Stokes signals under either normal or pumping conditions. This was already briefly highlighted in ref. 11 and is one of the main points we want to raise in this paper. We highlight first a few points around this issue:

- The distribution of SERS enhancements translates in a distribution for the Stokes cross-section σ_S. From there, it is then convenient to obtain the anti-Stokes cross-section as $\sigma_S = A\sigma_S$, where A is the asymmetry factor defined in eqn (1).
- The physical origin of A is a combination of the intrinsic electronic resonances of the molecule (which are the same for all identical molecules on the substrate) and the underlying electromagnetic (plasmon) resonance profile. This second contribution is *a priori* dependent on the molecule position and should therefore be described by a probability distribution, which may be independent or correlated with σ_S.
- We can simplify this problem thanks to two key arguments: (i) the plasmon resonances are typically wide compared to the energy separation between Stokes and anti-Stokes peaks, and A is therefore not expected to vary widely; (ii) on the contrary, due to the long-tail distribution of enhancements, the variations of σ_S across the sample are huge (many orders of magnitude), and therefore overwhelms any small variation that may occur in A. We therefore make the assumption that A is to a first approximation constant: $A \approx \bar{A}$.

From there, we can now study the averaging of the Stokes and anti-Stokes signals. In the thermally dominated regime (Boltzmann factor dominating in eqns (3) and (4)), both Stokes and anti-Stokes signals are proportional to $\sim\langle\sigma_S\rangle$. In the pumping dominated regime (where the first term in eqns (3) and (4) dominates), the Stokes signal is still proportional to $\langle\sigma_S\rangle$, but the anti-Stokes signal is now proportional to $\propto\langle\sigma_S{}^2\rangle$. This is because anti-Stokes vibrational pumping is essentially a two-photon process. A long-tail distribution of enhancements has therefore dramatic consequences in the comparison between the averages of $\langle\sigma_S\rangle$ and $\sqrt{\langle\sigma_S^2\rangle}$. In ref. 11, for example, we showed in an example that $\langle\sigma_S{}^2\rangle/\langle\sigma_S\rangle$ is close to the maximum available enhancement (only smaller by a factor of $\sim$2), while the average $\langle\sigma_S\rangle$ is typically 100–500 times smaller than this maximum. As a result of this, *the anti-Stokes signal in the pumping regime is heavily biased towards the sites with the largest enhancements*, and it comes from a very different averaging process than the Stokes counterpart. This was already pointed out in ref. 1.

1.4 Photobleaching as a probe of the enhancement distribution

Ultimately, the outcome of an experiment is that an intensity is measured for either the Stokes or anti-Stokes signals of a peak at a given temperature T. The measured signal is already the averaged contribution of many molecules subject to a long-tail distribution. Doubtlessly, it is not easy to backtrack from the integrated values of the intensity to demonstrate that the signals are being averaged in different ways over the probability distribution of enhancements, because what is measured is already averaged and affected by additional parameters of the problem (like the asymmetry factor A, or the lifetime τ). We therefore need an additional tool to modify in some way this enhancement distribution.

This is where the photostability of the probe can provide an additional insight into the problem. It is a well known experimental fact that photobleaching in SERS may occur under certain conditions (which depend primarily on the combination of the probe, the laser excitation wavelength, and the power density). Moreover, since photobleaching has generally an electromagnetic origin (it starts with absorption of a photon), it is also reasonable to assume that the photobleaching rate is linked to the electromagnetic (EM) enhancement and therefore to the SERS enhancement F. Following this line of reasoning, one would also argue that the higher the EM or SERS enhancement, the faster the photobleaching. Photobleaching is a well-known issue in SERS and these simple arguments are usually implicitly accepted (although very rarely supported explicitly by experimental evidence).

Assuming that these facts are true, the photostability of the probe provides us with exactly the tool we need. It modifies the enhancement distribution as a function of time, simply by destroying the molecules with the highest enhancements, for which the bleaching rate is the fastest. It can therefore be used as a tool to probe the SERS enhancement factor distribution (this was in fact already suggested in ref. 11). A simple extrapolation of these facts to the vibrational pumping problem suggests that *anti-Stokes signals under vibrational pumping conditions should bleach at a different rate from the Stokes counterparts*. In fact, we can close the circle by using this as an experimental confirmation that the bleaching rate is linked to the enhancement.

The rest of the paper is devoted to an experimental proof of these facts. By the same token, the results shown in the following section highlight the underlying meaning of the cross-sections measured by this method, in particular with respect to the presence of a limited photostability of the probes. As we shall show from the experimental evidence here, the SERS vibrational pumping method provides an estimate of the cross-section which is the highest enhancement on the substrate that is also compatible with the photostability of the probe (at a given laser power density and over a prescribed observation time).

2. Experimental results

2.1 Temperature dependent pumping experiments

With the background of the previous subsections, we now address the question of how the estimation of cross-sections might be changed under the presence of photobleaching, and how that can be interpreted in terms of the averaging of the signal over the distribution of enhancements. In order to pursue this further, it is interesting to monitor *simultaneously* the Stokes and anti-Stokes intensity of a peak as a function of time (while it bleaches) at room temperature (in the ''normal'' or temperature dominated regime of section 1.2) and in the pumping regime at low temperatures. Measuring simultaneously the anti-Stokes and Stokes signals is achievable in some Raman systems with the use of low resolution gratings that allow a much wider window in energy on the CCD detector. This is even more favorable for low-energy modes which have, accordingly, a much smaller span between the Stokes and anti-Stokes sides and fit within the range of the CCD. We therefore choose, as a proof of principle, to monitor the 610 cm^{-1} mode of rhodamine 6G (RH6G) as a function of time and for different temperatures and laser power densities. All experiments are performed on samples of RH6G prepared as in ref. 1 and 2 with either (i) a Jobin Yvon LabRam confocal spectrometer equipped with a $\times 50$ long working distance objective and the sample in a Linkham cryostat for microscopy, or (ii) a Jobin Yvon U1000 double additive spectrometer with the sample in a closed-cycle cryostat with optical windows. We use three different laser excitations (633, 514, or 647 nm depending on the experiment).

At room temperature, all the modes are dominated by the second term in eqns (1), (3) and 4, and we have bleaching operating at the same time. Hence, if the bleaching rate is linked to the enhancement, we expect the molecules with the highest cross-sections in the tail of the distribution to disappear first. However, the disappearance of the high cross-section tail of the distribution, does not affect much the prefactor $\langle\sigma_{aS}\rangle/\langle\sigma_S\rangle \approx \bar{A}$ in eqn (4), which is approximately constant and independent of the enhancement factor. This of course does not mean that the anti-Stokes and Stokes signals themselves are stable. The intensity of both is bleached but keeping approximately the same ratio. This situation is explicitly shown in Fig. 2a, where the anti-Stokes and Stokes signals are seen to decay at room temperature (293 K) while keeping a constant ratio ~ 0.1. All the observed decays are non exponential, a fact that can easily be expected from the presence of a non uniform distribution of bleaching times associated with the different enhancements. We shall not study this aspect of the decays here since it is not directly related to vibrational pumping itself.

The situation is completely different at low temperatures (77 K) as shown in Fig. 2b. We know that in our experimental conditions we are in the pumping dominated regime at this temperature; we are now dealing with the first term in eqns (1), (3), and (4)). Photobleaching is still present and the signals decay over time, but ρ also decays over time now. The reason is that, as explained previously, the average anti-Stokes signal ($\propto\langle\sigma_S^2\rangle$) is much more heavily influenced by the highest enhancements in the distribution than the Stokes signal (($\propto\langle\sigma_S\rangle$)). Therefore, if photobleaching of the tail of the distribution (high SERS enhancements) happens first, the anti-Stokes signal decays much faster than the Stokes signal, as observed here. Moreover, the ratio ρ varies as $\langle\sigma_S^2\rangle/\langle\sigma_S\rangle$, which is approximately the largest cross-section in the distribution. The decay of ρ over time simply reflects the faster photobleaching of the molecules with the highest enhancements.

The presence of photobleaching affects the ratio in two completely different ways at high or low temperatures with the sample in two different regimes (pumping or thermally dominated). This effect can be seen most of the time in real time in the pumping regime where anti-Stokes and Stokes signals are seen to bleach but without preserving their relative intensities. This latter effect is even more dramatic under 514 nm laser excitation, where photobleaching for RH6G in SERS plays a more dominant role. The whole decay of the aS/S-ratio to negligible values in the pumping regime can happen in a matter of seconds for moderate to high power densities and, as before, there is a marked difference between the behaviors at

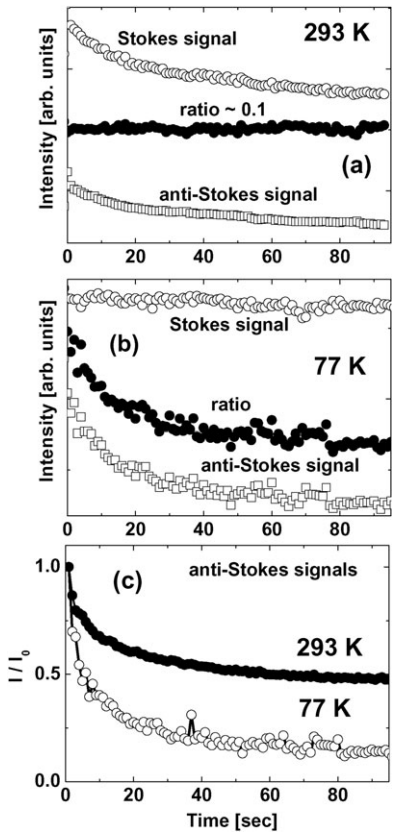

Fig. 2 A sample consisting of 0.5 μM of RH6G (with Ag colloids and 10 mM KCl) is dried on silicon, and measured in a Linkham cryostat for microscopy under a N_2 atmosphere. All data are with 3 mW of 633 nm laser excitation focused with a ×50 objective (~2 μm diameter spot) and 0.2 s integration time. The data is taken with a 600 lines mm^{-1} grating which allows the simultaneous measurement of the 610 cm^{-1} mode of RH6G on the Stokes and anti-Stokes sides. All the integrated intensities are background corrected and monitored in all cases for the same total amount of time. At room temperature (a), we are in the thermally dominated regime, and the anti-Stokes and Stokes signals are seen to decay while keeping their ratio approximately constant (~0.1). At 77 K (b) we are in the pumping dominated regime for these experimental conditions. The anti-Stokes signal decays much faster than the Stokes signal and this results in a time-dependent ratio ρ. We note that the Stokes signal also decays slower at 77 K compared to 293 K but this is related to the photobleaching effect itself and not to vibrational pumping. There are variations from point to point in the sample due to the inhomogeneity of the enhancement, but a rule of thumb is that the normalized (to $t = 0$) anti-Stokes signal decays much faster at 77 K than at 293 K as shown in (c), due to the different physical origin of the signals (vibrational pumping *vs.* thermal excitation), which implies a different averaging of the cross-sections.

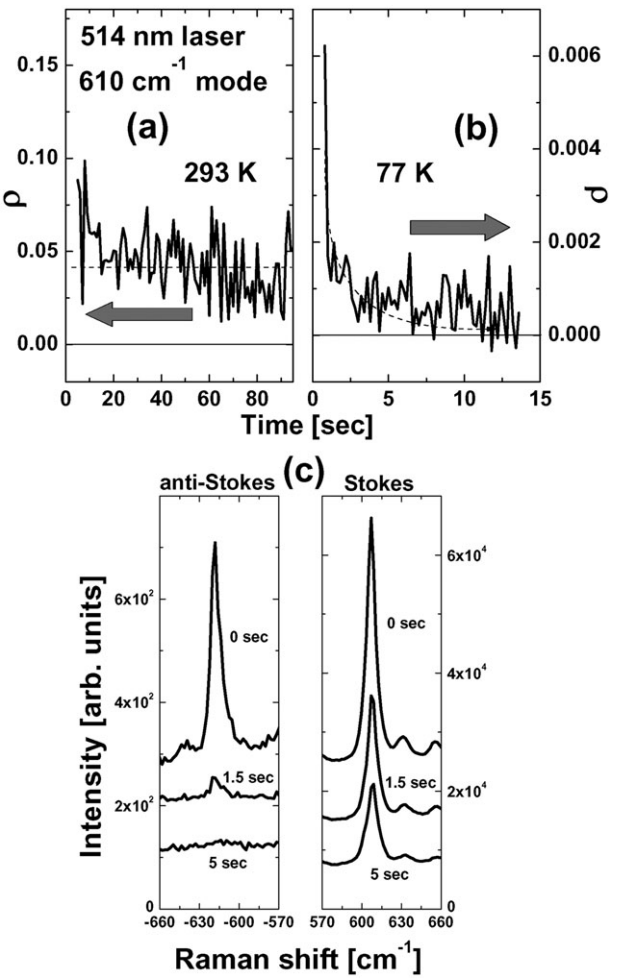

Fig. 3 Temporal dependence of the aS/S-ratios in the (a) thermally dominated (293 K) and (b) pumping dominated (77 K) regimes for 514 nm laser excitation. Measurements are performed under the same experimental conditions of Fig. 2 but for 5 mW incident power at 514 nm. The signal is strongly bleached at room temperature but the ratio remains finite and approximately constant over a period of more than 1 min. At 77 K, on the contrary, the ratio decreases to a negligible value in ~10 s. In (c) we further illustrate a unique phenomenon that only exists with the combination of SERS vibrational pumping and photobleaching: the disappearance of the anti-Stokes signal with a markedly different bleaching rate as its Stokes counterpart.

room and low temperatures. This is explicitly shown in Fig. 3. Fig. 3c illustrates further this unique phenomenon for Raman scattering, which only exists under SERS vibrational pumping conditions, *i.e.*: the disappearance of the anti-Stokes and Stokes signals with markedly different decay rates.

2.2 Power-dependent pumping experiments

Instead of the temperature dependent SERS pumping studies proposed in ref. 1 another possibility to estimate SERS cross-section *via* vibrational pumping comes from the *power dependence* of anti-Stokes and Stokes signals. As discussed extensively in ref. 1 and 2 and in the original report[7] the anti-Stokes signal is expected to raise quadratically with incident power while the Stokes signal remains linear. This produces a *linear* dependence of the aS/S-ratio in the pumping regime, which has been the subject of a considerable debate in the literature.[8,9] Ref. 1 and 2 established the conditions under which this effect can be observed reliably, without being confused with a laser-heating effect.[3]

Nevertheless, in view of the results presented in this paper so far, we need to inquire about the influence of the photostability of the probe in power dependence studies. The fact that the anti-Stokes signal is averaged differently over the enhancement distribution and that, accordingly, this results in a different

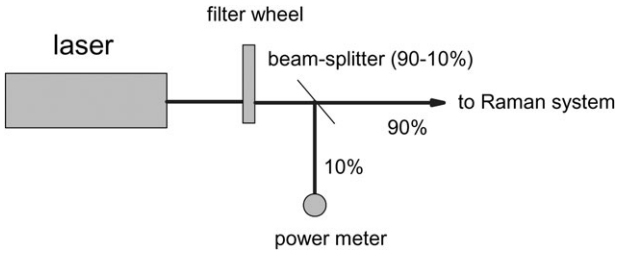

Fig. 4 A neutral density filter wheel and 10–90% beam-splitter are used to monitor the power constantly without any need to move the beam-path or the sample. For a fixed power, the signal is integrated for 1 s, which is then followed by a 5 s waiting period during which the laser power is changed to the next value with the filter wheel. In that manner, a time-dependent measurement is transformed into a power-dependence study. A high reproducibility is achieved and all the samples are exposed to exactly the same protocol of integration and exposure times to the laser.

photobleaching rate is a topic that needs to be addressed at the moment of estimating cross-sections from these signals. By the very nature of the technique, these are certainly strong candidates to produce different answers depending on the "memory" of how the experiment is carried out. We also expect to see qualitatively different scenarios in the two regimes of Fig. 1 (thermally or pumping dominated).

In view of the importance of keeping control of exposure time to the lasers to make them consistent and reproducible we devised a power dependence study using the simple setup shown schematically in Fig. 4. A neutral density filter wheel and a beam splitter allow for a precise change of power in the measurement as a function of time while a reading (proportional to the power and previously calibrated) can be obtained at all times through a power meter and the beam-splitter. In this manner, all measurements can be performed with exactly the same protocol of integration and exposure times without unnecessary interruptions or unwanted exposures. The caption in Fig. 4 provides a few further details.

Fig. 5 shows the basic results, which we summarize here:

• At room temperature, Stokes and anti-Stokes signals rise linearly at low power densities and eventually depart from linearity, as shown in Fig. 5a. The departure from linearity happens at different power levels depending on the combination of integration and exposure time. When a characteristic time (which depends on the history of the sample: integration time, accumulated exposure time, and power densities) is smaller than the photobleaching decay time, a linear dependence of the signal is observed. Beyond a certain power density, the loss of signal due to the increasing photobleaching rate overcomes the increase in intensity produced by the higher laser power and the response is sub-linear. Despite having an obvious influence from photobleaching in the data (that can be seen with a naked eye) the aS/S-ratio remains approximately constant in the same range, as seen in Fig. 5b. The averages over the distribution of enhancement for the Stokes and anti-Stokes signals are affected by the same amount under the presence of photobleaching at room temperature. They are both proportional to $\langle \sigma_S \rangle$.

• At $T = 10$ K, *i.e.* in the pumping regime, the situation is completely different. The anti-Stokes signal rises quadratically at very low laser power densities, while the Stokes signal is proportional to I_L, as seen in Fig. 5c. This produces an initial aS/S-ratio dependence that is linear in I_L as shown in Fig. 5d. However we have again the interplay between the integration

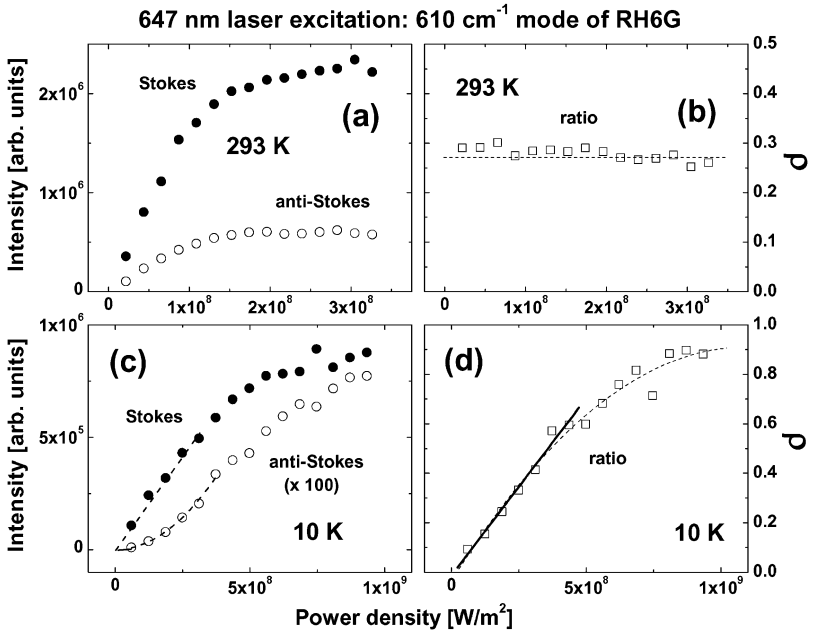

Fig. 5 Power dependence of the anti-Stokes and Stokes signals of the 610 cm^{-1} mode of RH6G at (a) 293 K and (c) 10 K for 647 nm excitation (Kr^+-ion laser). The corresponding ratios are shown in (b) and (d), respectively. Measurements are performed under the same experimental conditions reported in ref. 1 and 2 together with the added setup shown in Fig. 4. All measurements are for 1 s integration time with a 5 s interval in between measurements (exposing the sample to the laser) to adjust the power to the next value. At low temperatures the photostability is better and measurements can be carried out up to slightly higher powers (note the change in the horizontal scale in (c) and (d)).

+ exposure times competing with the power-dependent photobleaching rate. At some point, the quadratic and linear dependencies of the signals are lost, and the aS/S-ratio goes sub-linear. This is because the anti-Stokes signal, proportional to $\langle\sigma_S{}^2\rangle$ is affected more by the photobleaching process than the Stokes one, proportional to $\langle\sigma_S\rangle$. This is another manifestation of the same effect already discussed in the previous section and illustrated in Fig. 2 and 3.

Extracting cross-sections from the power dependence is very convenient because it avoids lengthy temperature scans but with the caveat that we cannot avoid the influence of photobleaching, for some probes, if the exposure time is too long or the power density too high. The presence of photobleaching has the same consequences as for the cross-sections extracted from the temperature scans. The measured cross-section is that of the molecules with the highest SERS enhancement *and* that have not yet photobleached. Depending on the exact experimental procedures, one may not measure the highest SERS enhancement on the sample if those molecules have already photobleached.

Fig. 6a and b show two examples to illustrate this point for two different laser excitations (514 and 647 nm) at $T = 10$ K. We monitor the anti-Stokes signal of the 610 cm^{-1} mode of RH6G using a short integration time (1 s) and a delay time of 5 s in between points. The full measurement takes a total of 36 s and this is well within the region where the combined

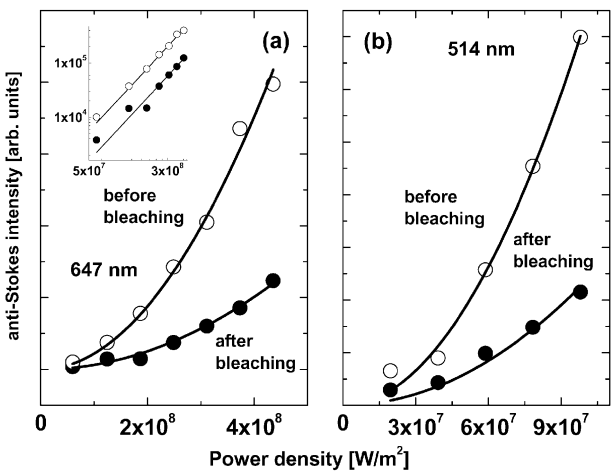

Fig. 6 Anti-Stokes signals at $T = 10$ K for two different laser excitations: (a) 647 nm, and (b) 514 nm. Both measurements are performed in the low-power density region where the anti-Stokes signal is quadratic with incident power (as revealed, for example, in a log–log plot in the inset of (a) in which the data have a slope of 2 ± 0.1). The measurement is done with the shortest possible integration and exposure times (1 s integration time and 5 s interval in between points). After the last point is taken, the sample is left for 15 min exposed to the laser. The power is turned off afterwards and the measurement is repeated. A parabola with a much smaller coefficient implies an overall smaller cross-section. Even when photobleaching does not affect much the measurements themselves because of the low power level and the short integration time, the accumulated effect of the exposure time in between the two can be clearly seen. An estimation of cross-sections from these data can give two completely different answers depending on the interplay between photobleaching, integration, and exposure times.

integration + exposure times and power densities make photobleaching effects negligible. A clear quadratic dependence (shown on a log–log plot in the inset of Fig. 6a with a slope of 2 ± 0.1) can be seen. At the power level of the last point, we then wait for 15 min exposing the sample to the laser. This is sufficient here to trigger some photobleaching, at least for some molecules, presumably those with the highest SERS enhancement. Subsequently, we come down to zero power and start the same measurement again. This is the difference between the "*before bleaching*" and "*after bleaching*" curves in Fig. 6a and b. The power dependence of the anti-Stokes signal is still quadratic as before; *i.e.* we are in the "safe" region as far as the photobleaching rate is concerned during the second measurement, but the extracted cross-section is smaller. This is simply the highest cross-section of the molecules that have survived the 15 min photobleaching step. This illustrates clearly the fact that the sample has a memory of the exposure to the laser and the accumulated photobleaching. It should be emphasized here that "memory to exposure" means always a process of degradation of the signal in the spot area exposed to the laser. In our experimental conditions, the signal never recovers to its original value. This highlights the extreme care that has to be taken when assessing the possible effects of photobleaching for the cross-section estimation using SERS vibrational pumping, because the technique (in one of its possible implementations, when the power dependence of the anti-Stokes signal is studied) is unavoidably linked to the use of laser power dependencies. The interplay in the experimental procedure among integration time, laser power density, exposure time, and photobleaching rate needs to be properly mapped out to obtain consistent cross-sections.

3. Discussion and conclusions

This paper attempts to move forward our understanding of SERS pumping and the factors that affect how we quantify and measure cross-sections.[1,2] We focus in particular on the inevitable presence of a distribution of enhancements, which is in most cases a long-tail distribution, and on its intricate relation with the possible limited photostability of the probe.

Our results lead to a number of important conclusions and comments:

• The results presented in Fig. 2, 3 and 6 are the clearest experimental evidences (that we are aware of) showing that *the photobleaching rate is linked to the enhancement*: the bleaching rate is larger for the larger enhancements. This is a key result of this paper and a result which is sometimes assumed or taken for granted without any real experimental evidence. Here, we have a population of molecules with a distribution of enhancement factors and two signals that arise from different averaging processes over the distribution; one giving more prevalence to the highest enhancements than the other. The experimental conditions are otherwise identical for the whole population and the signals are monitored *simultaneously*. Yet, the anti-Stokes signal decreases at a much faster rate in Fig. 2 and 3, showing that the initial step in the photobleaching path is linked to the enhancement. The same conclusion can be reached from a different viewpoint from the data in Fig. 6.

• It is also obvious from these experimental data that if vibrational pumping (using either the plateau region in Fig. 1 or the power dependence in Figs. 5d or 6) are used for an estimation of SERS cross-sections, the outcome would be strongly influenced by any photobleaching. The presence of photobleaching must therefore be carefully monitored and avoided by an appropriate adjustment of the experimental conditions. If this is not done (or is not possible), the exact experimental procedures (and in particular the exposure and integration times) will intimately be related to the outcome of the experiment together with the intrinsic photostability of the probe.

• In fact, the presence of photobleaching during the estimation of SERS cross-sections with vibrational pumping could possibly be viewed as an advantage. The temporal variation of the ratio at low temperatures (Fig. 2b and 3c) is an indirect measure of how the ''uppermost edge'' of the distribution of enhancements[13] bleaches with respect to the average. One could therefore conceive SERS vibrational pumping experiments where photobleaching is carefully controlled, so that the time dependence of the aS/S ratio can be used to determine the SERS enhancement distribution. A similar type of information can be extracted following the experimental scheme used for the data of Fig. 6. The quantitative interpretation of these types of experiments in terms of enhancement distributions would however still require a better understanding (theoretical and experimental) of the exact link between photobleaching rate and SERS enhancement.

• Finally, it is worth mentioning that one could also ask about the possible role of vibrational pumping itself in the photostability (vibrational dissociation[14]), but the average population achieved in the levels under typical SERS pumping conditions[1,2] is much too small to justify this as a possible photobleaching pathway. The bulk of the experimental evidence at this time suggests an electronic mechanism linked to the electromagnetic enhancement.

Overall, our results here demonstrate that photobleaching in SERS vibrational pumping is a controllable, and sometimes even advantageous, aspect of the problem. A realistic approach for applications is to try to understand the possible consequences of a distribution of enhancements in combination with the limited photostability of the probes, and incorporate this understanding in the design of protocols that can help in the comparison among different experimental conditions, as well as in the estimation of SERS cross-sections and enhancement factors. Unlike what happens under normal Raman spectroscopy conditions, the anti-Stokes/Stokes ratio is *not* a self-normalizing quantity (with respect to photobleaching) in the pumping regime because both signals are affected differently by the averaging. This provides a unique tool to study photobleaching in SERS itself but, at the same time, it suggests that for the purpose of quantifying the cross-section the presence of photobleaching must be minimized as much as possible and proper experimental protocols must be in place to compare relative efficiencies of different substrates.

Finally, our results also confirm two specific aspects of our previous studies in vibrational pumping: (i) that the anti-Stokes signal is averaged differently from the Stokes counterpart over the distribution of enhancements; and (ii) that vibrational SERS pumping provides estimates of the cross-sections which are biased towards the highest enhancements available in the distribution; with the latter being compatible with the photostability of the probe under given experimental conditions and procedures.

Acknowledgements

P.G.E. and E.C.L.R. acknowledge financial support from the Royal Society of New Zealand (RSNZ) through a Marsden Grant.

References

1 R. C. Maher, L. F. Cohen, E. C. Le Ru and P. G. Etchegoin, *J. Phys. Chem. B*, 2006, **110**, 19469.
2 R. C. Maher, P. G. Etchegoin, E. C. Le Ru and L. F. Cohen, *J. Phys. Chem. B*, 2006, **110**, 11757.
3 R. C. Maher, L. F. Cohen, E. C. Le Ru and P. G. Etchegoin, *Faraday Discuss.*, 2006, **132**, 77.
4 E. C. Le Ru and P. G. Etchegoin, *Faraday Discuss.*, 2006, **132**, 63.
5 R. C. Maher, L. F. Cohen, J. C. Gallop, E. C. Le Ru and P. G. Etchegoin, *J. Phys. Chem. B*, 2006, **110**, 6797.
6 M. Moskovits, *Rev. Mod. Phys.*, 1985, **57**, 783.
7 K. Kneipp, Y. Wang, H. Kneipp, I. Itzkan, R. R. Dasari and M. S. Feld, *Phys. Rev. Lett.*, 1996, **76**, 2444.
8 A. G. Brolo, A. C. Sanderson and A. P. Smith, *Phys. Rev. B*, 2004, **69**, 045424.
9 T. L. Haslett, L. Tay and M. Moskovits, *J. Chem. Phys.*, 2000, **113**, 1641.
10 B. Pettinger, in *Surface-Enhanced Raman Scattering: Physics and Applications (Topics in Applied Physics Vol. 103)*, ed. K. Kneipp, H. Kneipp and M. Moskovits, Springer Verlag, Berlin, 2006, p. 217.
11 E. C. Le Ru, P. G. Etchegoin and M. Meyer, *J. Chem. Phys.*, 2006, **125**, 204701.
12 The enhancement factor F here refers to the SERS enhancement factor in the so-called E^4-approximation discussed in detail in ref. 13.
13 E. C. Le Ru and P. G. Etchegoin, *Chem. Phys. Lett.*, 2006, **423**, 63.
14 Y. R. Shen, *The principles of non-linear optics*, Wiley, New York, 1984.